Agricultural and Forest Meteorology 321 (2022) 108974

Contents lists available at ScienceDirect

Agricultural and Forest Meteorology

journal homepage: www.elsevier.com/locate/agrformet

Comparing sap flow calculations from Heat Field Deformation (HFD) and Linear Heat Balance (LHB) methods

Junbin Zhao [a,*], Holger Lange [a], Helge Meissner [a], Ryan M. Bright [b]

[a] Department of Biogeochemistry and Soil Quality, Division of Environment and Natural Resources, Norwegian Institute of Bioeconomy Research, Ås, Norway
[b] Department of Forest and Climate, Division of Forest and Forest Resources, Norwegian Institute of Bioeconomy Research, Ås, Norway

ARTICLE INFO

Key words:
Norway spruce
Sapwood depth
Sap flow density
Thermal conductivity
Reversed flow

ABSTRACT

Heat Field Deformation (HFD) is a widely used method to measure sap flow of trees based on empirical relationships between heat transfer within tree stems and the sap flow rates. As an alternative, the Linear Heat Balance (LHB) method implements the same instrumental configuration as HFD but calculates the sap flow rates using analytical equations that are derived from fundamental conduction-convection heat transfer theories. In this study, we systematically compared the sap flow calculated using the two methods based on data that were recorded using the same instrument. The measurements were conducted on four Norway spruce trees. We aimed to evaluate the discrepancies between the sap flow estimates from the two methods and determine the underlying causes. Diurnal and day-to-day patterns were consistent between the sap flow estimates from the two methods. However, the magnitudes of the estimated sap flow were different between them, where LHB resulted in much lower estimates in three trees and slightly higher estimates in one compared to HFD. We also observed larger discrepancies in negative (reversed flow) than in positive sap flow, where the LHB resulted in lower reversed flow than HFD. Consequently, the seasonal budget estimated by LHB can be as low as ~20% of that estimated by HFD. The discrepancies can be mainly attributed to the low wood thermal conductivities for the studied trees that lead to substantial underestimations using the LHB method. In addition, the sap flow estimates were very sensitive to the value changes of the empirical parameters in the calculations and, thus, using a proper case-specific value is recommended, especially for the LHB method. Overall, we suggest that, despite the strong theoretical support, the correctness of LHB outputs depends largely on the tree individuals and should be carefully evaluated.

1. Introduction

Sap flow is an important process in trees that transports water from the soil to the atmosphere. Sap flow is generally used to estimate tree water use and indicate the functionality of trees especially under environmental stresses (e.g., Becker, 1996; Kume et al., 2007; O'Brien et al., 2004). To measure the tree sap flow, many thermodynamic methods have been developed in the last few decades (Smith and Allen, 1996). These methods are mostly based on empirical relationships between heat transfer within tree stems and the corresponding sap flow rates.

As one of the thermodynamic methods, the Heat Field Deformation (HFD) approach (Cermak et al., 2004) has been applied to measure sap flow of different tree species (e.g., Børja et al., 2013; David et al., 2012; Nadezhdina et al., 2018). The HFD design is composed of one needle-like heater inserted in the sapwood and three temperature sensors placed above, below and at the side of the heater, respectively, inside the sapwood (Nadezhdina et al., 2012). The HFD method has the advantages of being able to 1) continuously measure sap flow at a high temporal resolution, 2) measure the reversed flow, and 3) measure sap flow in multiple depths of the sapwood at the same time. Despite the advantages of the HFD method, the sap flow calculation is still purely empirical, and, thus, its performance will still need to be evaluated against other methods on trees of various forest ecosystems.

Using the same instrumental configuration as the HFD, the Linear Heat Balance (LHB) method was introduced by Trcala and Cermak (2016). The LHB method calculates the sap flow using analytical equations that are derived from fundamental conduction-convection heat transfer theories. The LHB-calculated sap flow rates from an individual Douglas fir (*Pseudotsuga menziesii*) tree were briefly compared with those calculated from HFD over a window of 23 summer days (Trcala and

* Corresponding author at: Norwegian Institute of Bioeconomy Research: Norsk Institutt for Biookonomi, Postboks 115, N-1433 Ås, Norway
E-mail addresses: junbin.zhao@nibio.no, junbinzhao1985@gmail.com (J. Zhao).

https://doi.org/10.1016/j.agrformet.2022.108974
Received 19 November 2021; Received in revised form 11 March 2022; Accepted 22 April 2022
Available online 27 April 2022

Cermak, 2016). While the two methods showed good agreements in diurnal patterns, values calculated from HFD tended to have a much lower magnitude than those from LHB in the surface sapwood layers. However, in deeper layers, values from LHB were also lower than those from HFD during the daytime, which appeared to be associated with low wood thermal conductivities (Trcala and Cermak, 2016). Given the large discrepancies between the outputs from the two methods, their performance needs to be further evaluated with more tree samples and, importantly, the underlying reasons for the discrepancies will need to be investigated.

In this study, we measured sap flow from four Norway spruce (*Picea abies*) individuals using the HFD sensor configuration and calculated sap flow density based on both HFD and LHB methods. By comparing the sap flow calculated using the two methods, we aimed to answer the following questions: 1) Are the sap flow densities (SFD) calculated using HFD and LHB comparable to each other? 2) How different are the seasonal sap flow budget estimates computed from the two methods? 3) How does the choice of the empirical parameter values in the two methods affect the sap flow estimates? Because we have no independent observational reference, we discuss our findings in the context of sap flow reported elsewhere for the same species but using different methods. The results from the study improve our understanding of the reliabilities of the two methods by identifying the sources of uncertainties and point to future research directions for improving the two methods.

2. Methods and materials

2.1. Study site

The study was carried out at a forest site in Hurdal municipality (60°22′20" N, 11°4′42" E, 284 m a.s.l.), in southeast Norway. The site is dominated by Norway spruce (*Picea abies* (L) Karst.) with a tree density of 600 stems/ha and a mean tree height of 25 m. The trees vary in ages from 5 to 100 years, with a median age of 93 years in 2020. No active management activities are carried out at the site. The long-term mean annual temperature and precipitation are 3.7°C and 845 mm, respectively. The soils are podzolic in the upper part and hydrogenic (partially waterlogged) in the lower part.

2.2. Sap flow measurements

The sap flow was measured at a 1 h interval using HFD8 Sap Flow Meters (ICT International Inc., Armidale, Australia) on four similar-looking Norway spruces trees with ages of around 65 years. The four trees form a close group with a maximum distance of 15 meters between them on rather flat terrain. The instrument units were installed at a height of ~1.6 m on the stems on August 22nd, 2019. Following the default configuration, the axial distance was 1.5 cm between the heater and the upper (or lower) temperature sensors, and the tangential distance was 0.5 cm between the heater and the side temperature sensor as recommended by the manufacturer. The temperature sensors were distributed along needle-like probes at depths of 0.5, 1.5, 2.5, 3.5, 4.5, 5.5, 6.5 and 7.5 cm under the stem surface. Solar panels (50 W) were used to charge the internal battery of each instrument unit. However, availability of sunlight at the site is not sufficient to warrant continuous heating. To reduce the power consumption of the instrument, the heaters were only turned on 10-min before each measurement. A heating power of 0.026 W cm^{-1} was used for the heater of each instrument unit.

2.3. Sap flow calculations

Sap flow density (SFD, cm^3 cm^{-2} h^{-1}) was calculated using the HFD approach as follows (Nadezhdina et al., 2006; Nadezhdina et al., 2012):

$$SFD = 3600 \cdot D \cdot \frac{dT_0 + dT_{s-a}}{dT_a} \cdot \frac{Z_{ax}}{Z_{tg}} \cdot L^{-1} \tag{1}$$

where D is the wood thermal diffusivity and a nominal value of 0.0025 cm^2 s^{-1} is suggested by Nadezhdina et al. (2012), and the factor 3600 converts values to hourly SFD. The temperature difference between the lower and upper sensors is defined as the symmetric temperature difference (dT_s,°C) and the temperature difference between the side and the lower sensors is defined as the asymmetric temperature difference (dT_a,°C). The temperature difference between the upper and the side sensors is thus calculated by $dT_s - dT_a$ (i.e., $dT_{s\text{-}a}$,°C). The term $\frac{dT_0+dT_{s-a}}{dT_a}$ in Eq. (1) is referred to as the HFD ratio (R). The variable dT_0, which is referred to as the K-value in Nadezhdina et al. (2012), is the value of dT_a or $|dT_{s\text{-}a}|$ at which zero sap flow occurs (i.e., $dT_s = 0$°C). The Z_{ax} and Z_{tg} are distances (cm) from the heater to the upper sensor and side sensor, respectively. The L is the sapwood depth (cm). In cases of reversed flow, which is determined by $dT_s<0$, the following equation was used (Nadezhdina, 2018):

$$SFD = -3600 \cdot D \cdot \frac{-dT_0 + dT_a}{dT_{s-a}} \cdot \frac{Z_{ax}}{Z_{tg}} \cdot L^{-1} \tag{2}$$

The same dataset was also used to calculate the SFD using the LHB approach (Trcala and Cermak, 2016):

$$dT_{s-a} = \frac{H}{2\pi \cdot \sqrt{\lambda_{ax} \cdot \lambda_{tg}}} \cdot \left[e^{\frac{c_w \cdot SFD \cdot Z_{ax}}{2 \cdot \lambda_{ax}}} \cdot K_0\left(\frac{c_w \cdot SFD \cdot Z_{ax}}{2 \cdot \lambda_{ax}}\right) - K_0\left(\frac{c_w \cdot SFD \cdot Z_{tg}}{2 \cdot \sqrt{\lambda_{ax} \cdot \lambda_{tg}}}\right)\right] \tag{3}$$

where H is the heat power along the heater (W cm^{-1}). The λ_{ax} and λ_{tg} (W cm^{-1} K^{-1}) are the thermal conductivities of wood in the axial and tangential directions, respectively. The c_w is specific heat of water (4.186 J g^{-1} K^{-1}). The K_0 indicates the modified Bessel function of the second kind of order zero and was computed using the "besselK" function in the program R 4.1.0 (R Development Core Team, 2021). As suggested by Trcala and Cermak (2016), $\lambda_{ax} = k \times \lambda_{tg}$, where k was assumed to be 2 and λ_{tg} is estimated using the following equation:

$$\lambda_{tg} = \frac{H}{-2\pi \cdot dT_0 \cdot \sqrt{k}} \cdot \ln \frac{\sqrt{k} \cdot Z_{tg}}{Z_{ax}} \tag{4}$$

Note that, compared to the original equation in Trcala and Cermak (2016), a negative sign appears in the denominator of Eq. (4) because dT_0 is defined as $|dT_{s\text{-}a}|$, instead of $dT_{s\text{-}a}$ in Trcala and Cermak (2016), when zero sap flow occurs given the configuration. Since λ_{tg} is a positive definite quantity, Eq. (4) sets a limit to the value of k (i.e., $k = 9$ in our case) where a solution can be obtained, indicating limited validity of the LHB approach in general. The Eq. (3) was then solved to find the root for SFD using the "uniroot" function in the program R based on the Newton-Raphson method. Due to the nature of the Bessel function, only positive values can be found as the SFD root. Therefore, to calculate the reversed flow ($dT_s<0$), the $dT_{s\text{-}a}$ in Eq. (3) was replaced by $-dT_a$ and the positive roots found for SFD were then converted to negative values to represent the reversed flow. Nonetheless, we still noted a fraction (17%, Table S1) of the cases that could not be solved using the LHB approach. These cases were associated with negative R values where $-dT_{s\text{-}a} > dT_0$ for positive sap flow or $dT_a > dT_0$ for negative sap flow. In these cases, Eq. (3) simply has no root since the right-hand side is bounded from below and above (i.e., it has a minimum of $-dT_0$ for vanishing SFD). These negative R values thus occurred only when small sap flow rates (as indicated by dT_s, see Fig. S1) were present. They were excluded in the data analyses and were assumed to have a SFD value of zero when calculating the tree-scale sap flow.

We only used sap flow data that were measured during the growing season (May-September) of 2020. Tree #1 only had data available from July 21, 2020. Diameters at breast height (DBH) of the four trees were 24.8 (#1), 23.5 (#2), 20.3 (#3) and 17.5 cm (#4). Their sapwood depths (L) were estimated to be 3.5 (#1), 3.8 (#2), 7.5 (#3) and 7.5 cm (#4),

Table 1
Summary of linear regressions for sap flow density ($cm^3\ cm^{-2}\ h^{-1}$) estimated using HFD (as dependent variable) at different sapwood depths as a function of sap flow density estimated by LHB (as independent variable).

			Depth (cm)							
Tree #	Sign		0.5	1.5	2.5	3.5	4.5	5.5	6.5	7.5
#1	Positive	Slope	4.72	4.45	4.63	5.16	-	-	-	-
		R^2	0.98	0.99	0.99	0.99	-	-	-	-
	Negative	Slope	7.37	6.69	5.93	5.68	-	-	-	-
		R^2	0.99	0.99	0.99	0.99	-	-	-	-
#2	Positive	Slope	2.91	2.17	2.56	3.25	-	-	-	-
		R^2	0.89	0.93	0.94	0.94	-	-	-	-
	Negative	Slope	3.12	3.17	3.22	4.06	-	-	-	-
		R^2	0.84	0.95	0.96	0.98	-	-	-	-
#3	Positive	Slope	1.02	0.98	0.85	0.78	0.87	0.92	0.73	0.81
		R^2	0.89	0.9	0.96	0.96	0.97	0.94	0.94	0.96
	Negative	Slope	2.05	2.05	1.78	1.62	1.62	1.64	1.6	1.5
		R^2	0.98	0.98	0.99	0.98	0.98	0.97	0.98	0.98
#4	Positive	Slope	1.93	1.78	1.68	1.92	2.33	2.82	3.22	3.54
		R^2	0.95	0.97	0.97	0.97	0.96	0.97	0.98	0.98
	Negative	Slope	4.05	4.36	4.38	4.64	4.76	4.93	4.52	5.53
		R^2	0.99	0.99	0.99	0.99	0.99	0.99	1.00	0.99

respectively, based on the radial profiles of HFD ratios, which were adapted from the sap flow radial profiles as suggested in Nadezhdina (2018) (see details in supporting information Fig. S2). The sap flow data measured at depths that were greater than the estimated sapwood depths were not used (i.e., depths ≥4.5 cm for trees #1 and #2).

2.4. Data analysis

We conducted linear regressions between SFD values calculated from HFD (SFD_{HFD}) and LHB (SFD_{LHB}) to compare the outputs from the two methods. Since both methods assume the same zero sap flow point (i.e., $dT_s = 0°C$), the intercepts in the linear regressions were forced to be 0. The regressions were conducted separately for different trees, sapwood depths and signs of the SFD values (positive versus negative). To compare the diurnal patterns of SFD_{HFD} and SFD_{LHB}, SFD values were averaged over the entire season and plotted against the corresponding time of the day. We also computed sap flow budgets at the tree scale by multiplying SFD with the corresponding area of the concentric annulus at each depth (except those that were deeper than the sapwood depth) assuming a perfect circular stem and then summing the sap flow for all annuli. Since negative SFD values indicate hydraulic redistribution within trees (Nadezhdina et al., 2010) rather than downward sap flow

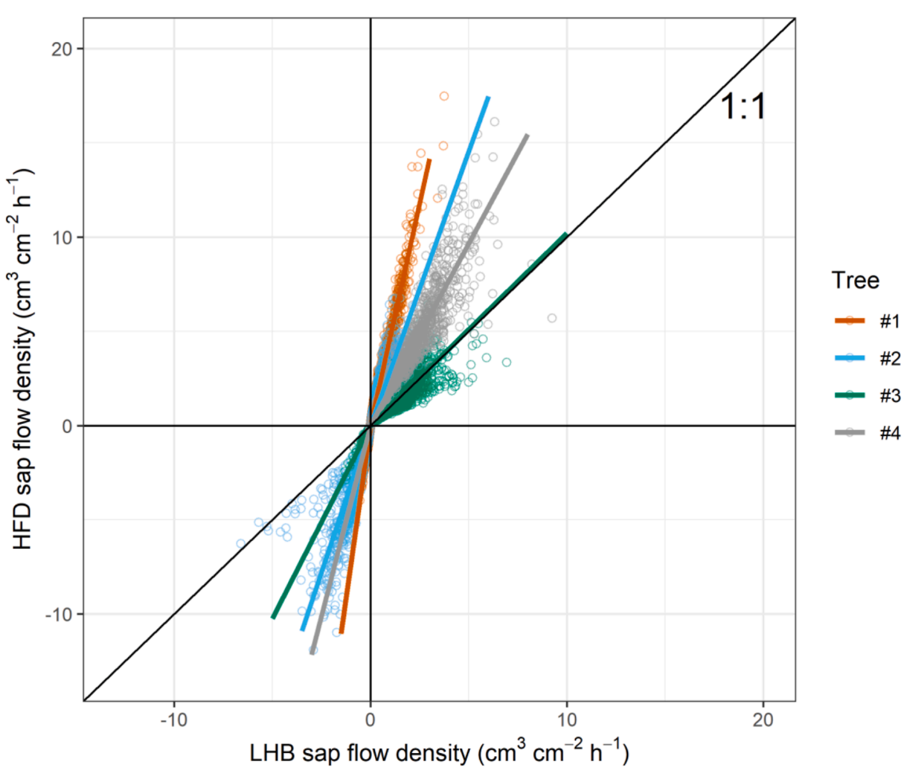

Fig. 1. Linear regressions of HFD-calculated sap flow density as a function of LHB-calculated sap flow density for the four studied trees at the depth of 0.5 cm into the stem.

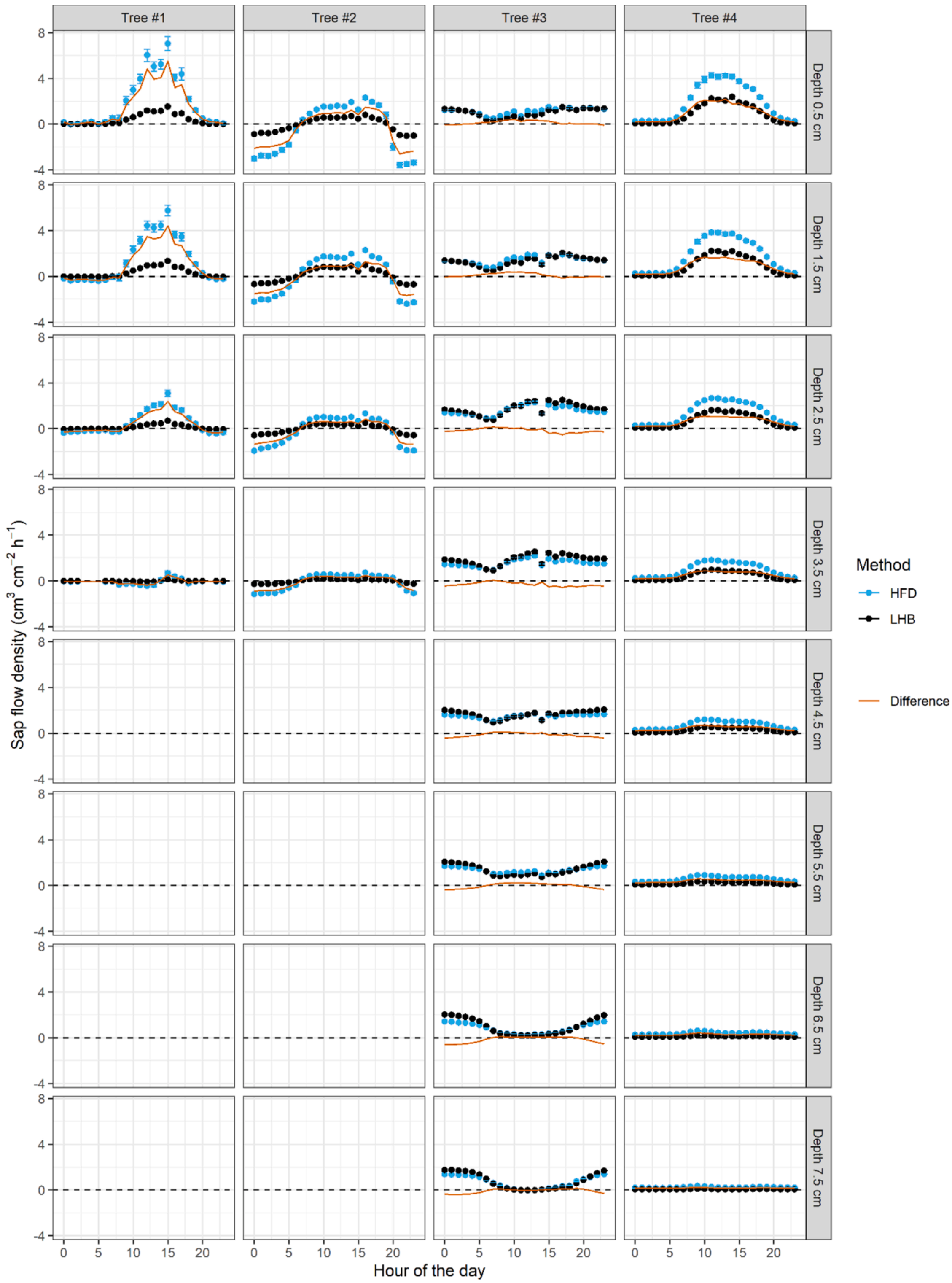

Fig. 2. Mean (± SE) diurnal variation of the sap flow density estimated using the HFD and LHB methods at different depths into the stem for the four trees over the entire study period (May-September 2020). Note that some SE values are smaller than the size of the symbols used for the mean values. The red lines indicate differences between the sap flow density values estimated using the two methods. For tree #1 and #2, depths that are ≥ 4.5 are out of the sapwood and the data were, therefore, not shown.

into the soil, they were excluded in the sap flow budget estimation.

Both HFD and LHB methods involve empirical parameters (i.e., k in LHB and D in HFD) that are associated with simple assumptions and thus may result in uncertainties in their outputs. To test how the change of these parameters could affect the discrepancies between the sap flow estimated by the two methods, we tuned the parameters across certain ranges (i.e., k: 1-3 and D: 0.0005-0.004 $cm^2 s^{-1}$) and calculated the SFD again. We took the slope in the linear regression between SFD_{HFD} and SFD_{LHB} as the ratio of SFD_{HFD} to SFD_{LHB} and investigated the slope changes when using different parameter values. To visualize the patterns, the nonparametric LOESS function was used to fit the slope values against the parameter values.

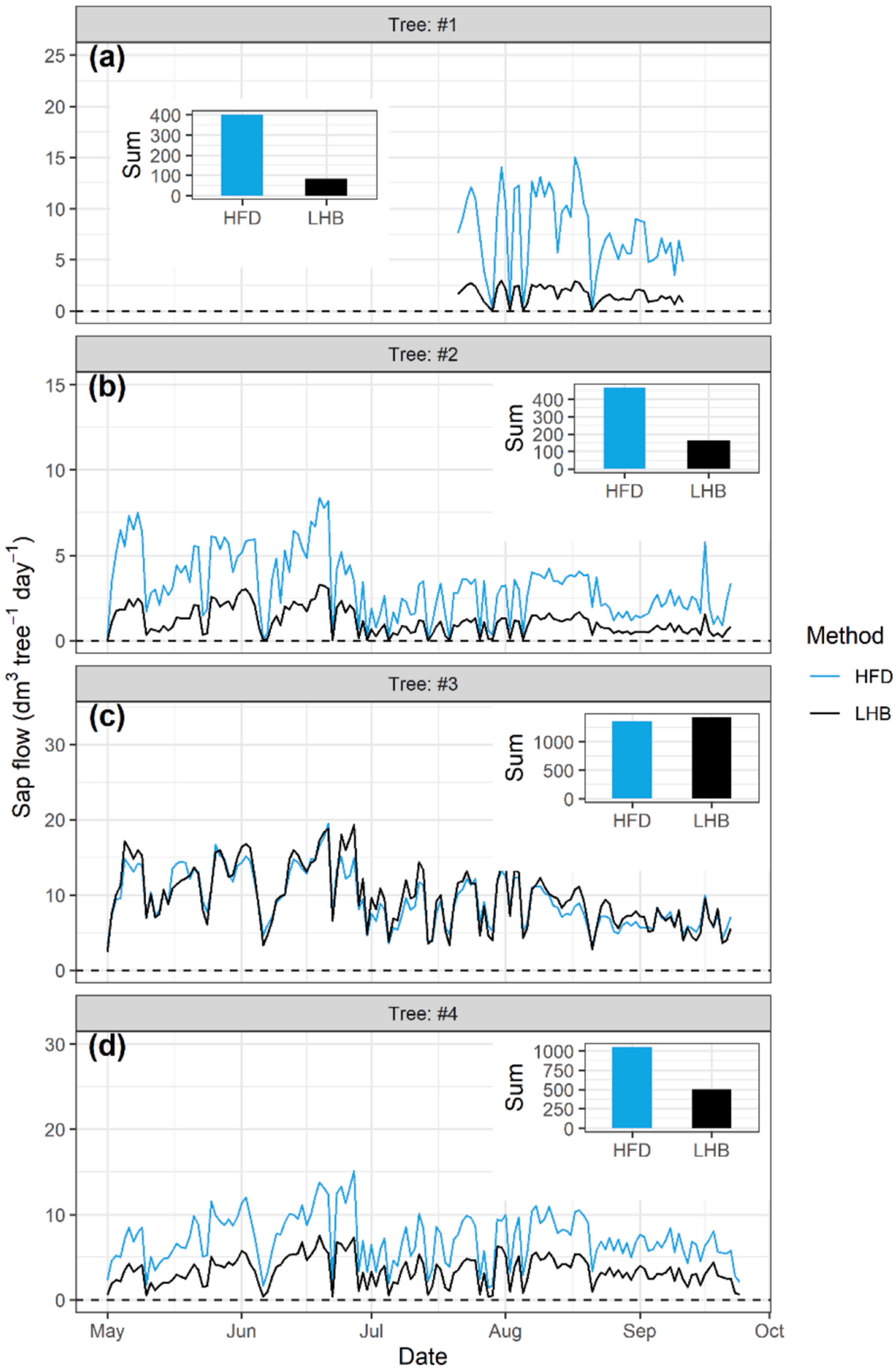

Fig. 3. Daily tree-scale sap flow estimated using HFD and LHB methods for the four trees over the growing season of 2020. Insets indicate the sums of the sap flow (dm^3) estimated based on the two methods over the entire period. Note that different scales are used for the y-axes.

All the data analyses were carried out in the program R 4.1.0 (R Development Core Team, 2021) and the graphs were prepared using the package “ggplot2” (Wickham, 2016). The code for calculating the sap flow density using both the HFD and LHB methods has been included in the R package “SapCal” that is freely available from Github (https://github.com/junbinzhao/SapCal).

3. Results

3.1. Linear regressions

The SFD estimated by HFD (SFD_{HFD}) showed strong linear relationships with those estimated by LHB (SFD_{LHB}) at all the depths along the sapwood for trees #1 and #4 (R^2 ranged from 0.95 to 1, Table 1, Fig. 1). For the tree #2 and #3, the relationships were relatively weaker (R^2 ranged from 0.84 to 0.99), especially at depths of 0.5 and 1.5 cm. Magnitudes of the estimated SFD values were substantially different between the two methods. The positive SFD_{LHB} values were much lower than SFD_{HFD} in tree #1 (regression slope: 4.45-5.16, Table 1), #2 (slope: 2.17-3.25) and #4 (slope: 1.78-3.54) but were slightly higher than SFD_{HFD} in tree #3 (slope: 0.73-0.98) except at the depth of 0.5 cm (slope: 1.02). Reversed flow (negative SFD) was observed in all the four trees. The magnitude of reversed flow was greater in SFD_{HFD} than in SFD_{LHB} in all the trees with regression slopes of 5.68-7.37 (#1), 2.12-4.06 (#2),

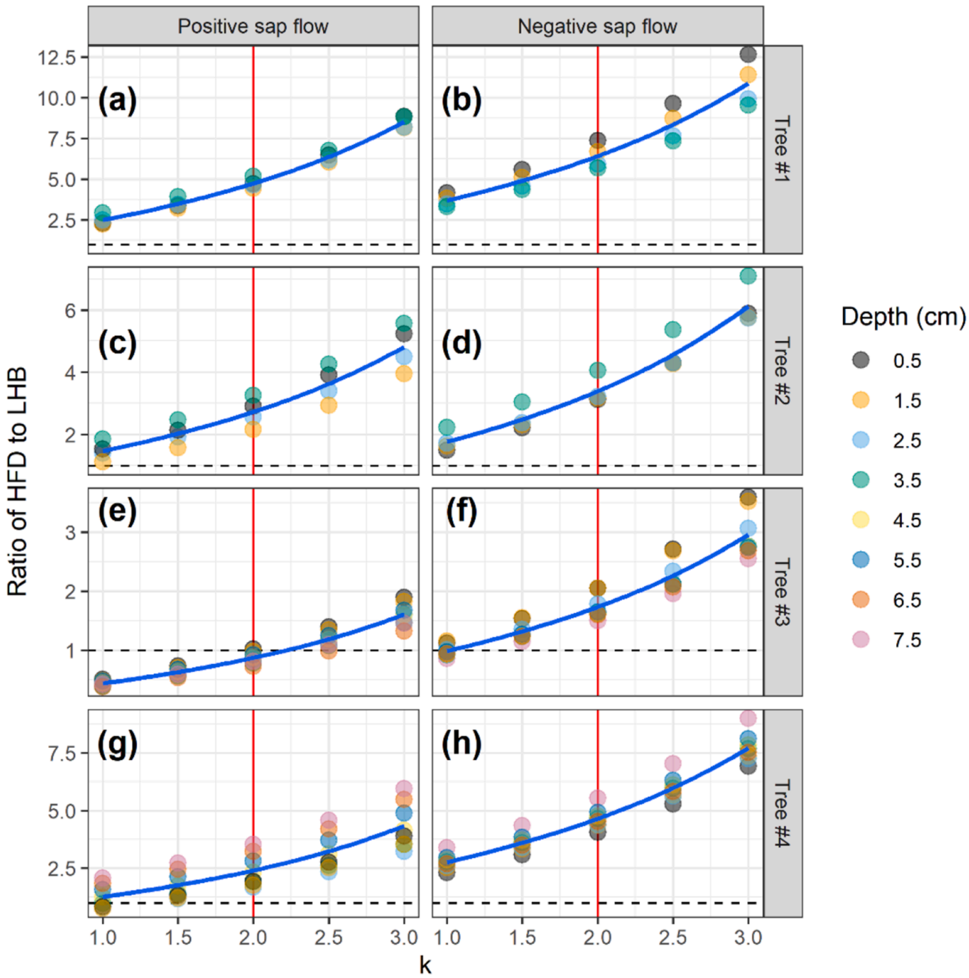

Fig. 4. Ratios of SFD_{HFD}: SFD_{LHB} as a function of the k-value in LHB method. The LOESS function is used to visualize the relationships as shown by solid blue lines. The red line indicates the default k-value used in the LHB method.

1.5-2.05 (#3) and 4.05-5.53 (#4). In general, the discrepancies between the two methods were much larger in negative SFD than in positive SFD.

3.2. Diurnal variations

For the trees #1 and #4, we noticed strong diurnal patterns in SFD where the peak SFD values were present between 10:00 and 15:00 (Fig. 2). The strength of the diurnal pattern declined along the sapwood depths. The diurnal patterns were generally consistent between SFD_{HFD} and SFD_{LHB}. Values of SFD_{HFD} were much higher than those of SFD_{LHB} and the differences were greater at the daytime when SFD was high and were much lower at the nighttime when SFD was close to zero. Overall, the difference reached as much as 5.5 $cm^3\ cm^{-2}\ h^{-1}$ in tree #1 (at the depth of 0.5 cm at 15:00) and 2.2 $cm^3\ cm^{-2}\ h^{-1}$ in tree #4 (at the depth of 0.5 cm at 13:00).

Tree #2 exhibited positive SFD values between 7:00 and 19:00 without obvious peaks while the average SFD values were negative across all the depths for the rest of the day (Fig. 2). During the daytime, SFD_{HFD} was higher than SFD_{LHB} and during the nighttime, the SFD_{HFD} was more negative than SFD_{LHB}, indicating that HFD generally resulted in larger values in both positive and reversed sap flow than LHB for the tree #2.

For the tree #3, the SFD diurnal pattern was different from other trees (Fig. 2). For the depths from 0.5 to 3.5 cm, peaks of SFD appeared between 10:00 and 17:00 while the lowest values were present at 7:00. At night, the average SFD mostly kept above 1 $cm^3\ cm^{-2}\ h^{-1}$. For the depths from 4.5 to 7.5 cm, nighttime SFD remained at similar levels as the outer layers of the sapwood, whereas the daytime SFD became much lower compared to the outer layers. SFD exhibited a decline after midnight and reached the lowest point between 10:00 and 15:00, where the values eventually dropped to zero at the depth of 7.5 cm. While the diurnal patterns were consistent between SFD_{HFD} and SFD_{LHB}, SFD_{HFD} showed lower values than SFD_{LHB}. Similar to trees #1 and #4, the differences between SFD_{HFD} and SFD_{LHB} were larger where larger SFD values were present for tree #3.

3.3. Seasonal variations and budgets

The daily sap flow fluctuated throughout the growing season with no strong seasonality for all the study trees (Fig. 3). The patterns agreed between sap flow values estimated by HFD and LHB. Among the four trees, tree #1 had the largest discrepancy between estimates from the two methods (Fig. 3a). This difference was reflected in the sap flow sums which differed by ~5 folds (403 and 84 dm^3 for HFD and LHB, respectively) in less than two months. For the tree #2, the seasonal budget was estimated to be 467 dm^3 by HFD whereas the estimate was 164 dm^3 by LHB (Fig. 3b). The tree #3 displayed the closest budget estimates by HFD and LHB where the values were 1359 and 1426 dm^3, respectively (Fig. 3c), which were higher than those of the other three trees. For the tree #4, the sap flow sum estimated by LHB (502 dm^3) was 48% of that estimated by HFD (1054 dm^3) (Fig. 3d).

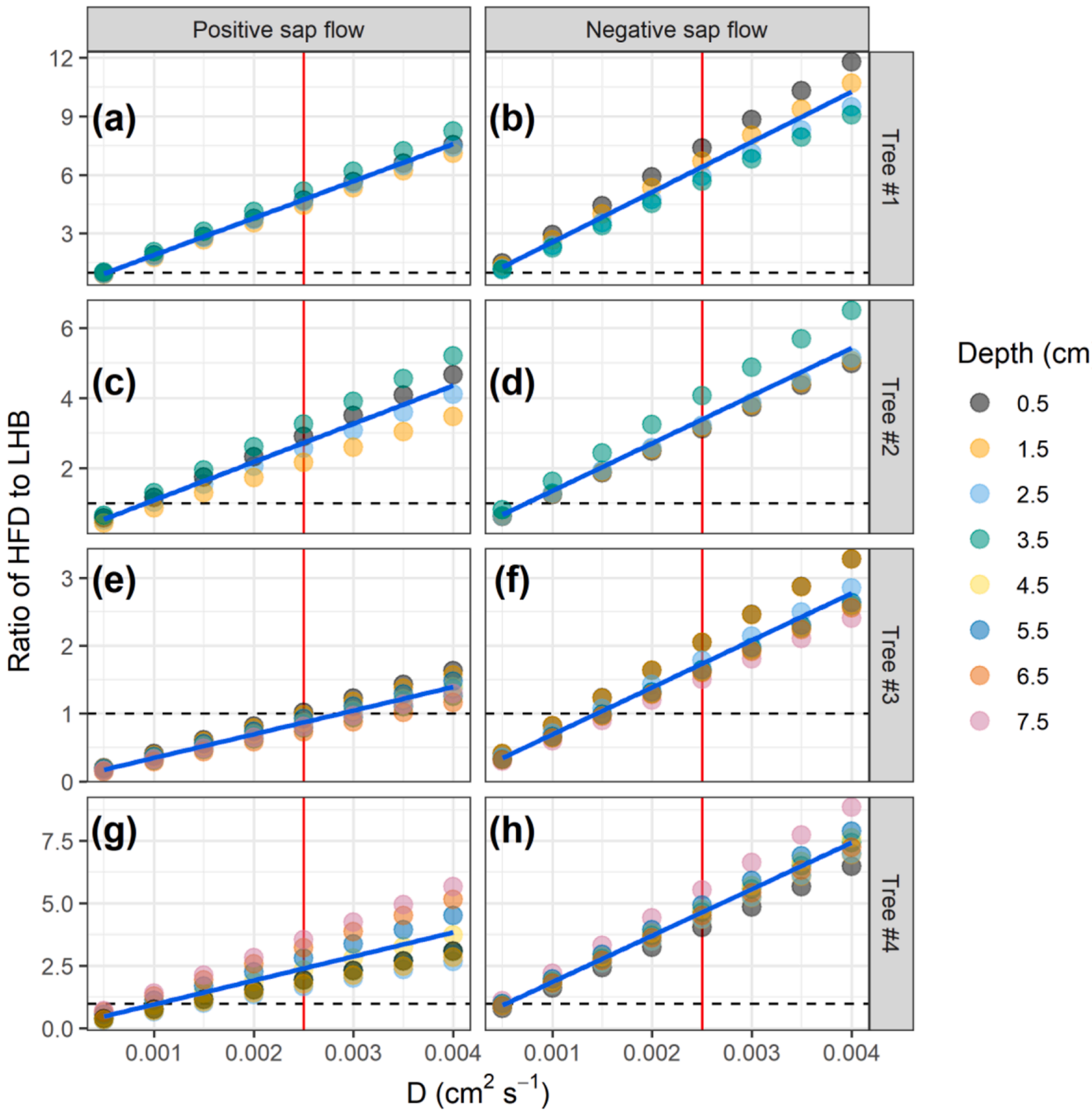

Fig. 5. Ratios of SFD_{HFD}: SFD_{LHB} as a function of the wood thermal diffusivity (D) used in the HFD method. The LOESS function is used to visualize the relationships as shown by solid blue lines. The red line indicates the default nominal value of D used in the HFD method.

3.4. Parameter tuning

Smaller k-values for LHB increased the estimated SFD_{LHB} values and, thus, reduced the ratio of SFD_{HFD}: SFD_{LHB} (Fig. 4). For tree #1, by reducing the k-value to 1 from the default 2, the SFD_{HFD}: SFD_{LHB} ratio only dropped to 2-4 (for both positive and negative sap flow) without achieving the SFD_{HFD}: SFD_{LHB} ratio of 1 (Fig. 4a, b). For tree #2, a smaller k-value of 1 resulted in a SFD_{HFD}: SFD_{LHB} ratio close to 1 for positive sap flow at the 1.5 cm depth but, for other depths and negative sap flow, a SFD_{HFD}: SFD_{LHB} ratio of 1 was not achieved within the chosen k-value range (Fig. 4c, d). By contrast, for tree #3, a larger k-value of 2.25-2.5 resulted in a SFD_{HFD}: SFD_{LHB} ratio that was the closest to 1 for positive sap flow (Fig. 4e) while, for negative sap flow, a smaller k-value of 1 was required (Fig. 4f). For tree #4, the lowest chosen k-value of 1 resulted in a SFD_{HFD}: SFD_{LHB} ratio of ~1 for positive sap flow (Fig. 4g) but not for negative sap flow (Fig. 4h).

When a greater value of D was used, the computed SFD_{HFD} became higher, which led to a higher ratio of SFD_{HFD}: SFD_{LHB} (Fig. 5). For tree #1, a small D-value of 0.0005 $cm^2\ s^{-1}$ led the SFD_{HFD}: SFD_{LHB} ratio to be around 1 for both positive and negative sap flow (Fig. 5a, b). The tree #2 required a D value of 0.00075-0.001 to achieve a SFD_{HFD}: SFD_{LHB} ratio of 1 (Fig. 5c, d). For the tree #3, the D-values of 0.003 and 0.0015 $cm^2\ s^{-1}$ were used to achieve the SFD_{HFD}: SFD_{LHB} ratio of 1 for positive and negative sap flow, respectively (Fig. 5e, f). The tree #4 required smaller D-values of ~0.001 and 0.0005 $cm^2\ s^{-1}$ for positive and negative sap flow, respectively, to have comparable SFD_{HFD} and SFD_{LHB} values (Fig. 5g, h).

4. Discussion

In this study, we systematically compared the tree sap flow that were estimated by two different methods, HFD and LHB, which use the same instrumental configurations. We found that the diurnal and day-to-day patterns were consistent between the sap flow estimates from the two methods, which agrees with Trcala and Cermak (2016). However, the magnitudes of the estimated sap flow were different between the two methods where LHB resulted in much lower SFD in three trees and slightly higher SFD in one compared to HFD (Table 1, Fig. 1). These results are not in line with the study of Trcala and Cermak (2016), who reported up to 2 times higher sap flow estimates by LHB than by HFD based on their 23-day measurement campaign on one Douglas fir tree. Overall, the seasonal budget estimated by LHB can be as low as only a

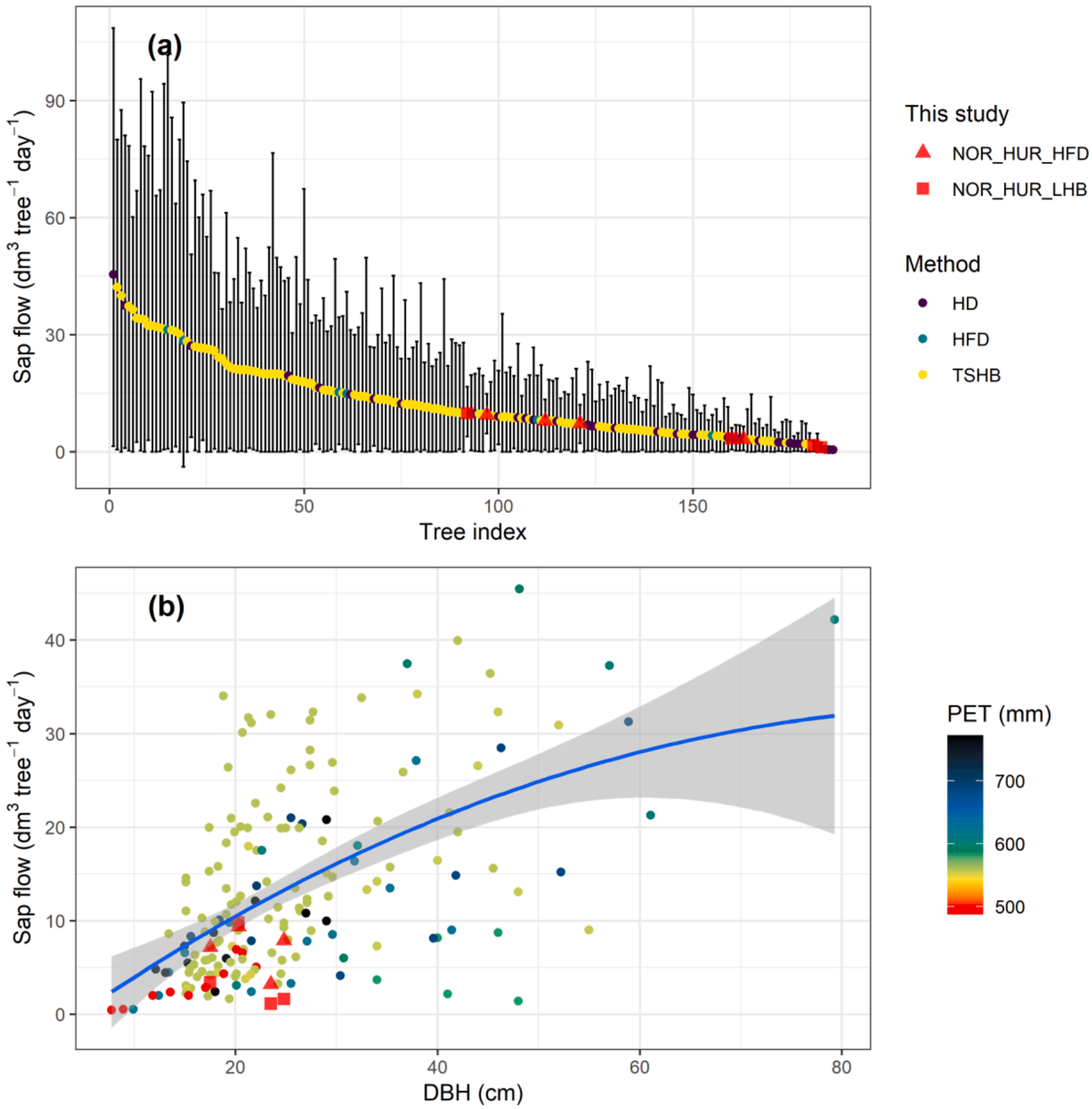

Fig. 6. Mean daily sap flow of Norway spruce trees (a total of 182 individuals) (a) and the sap flow values as a function of DBH (b). Error bars in (a) denotes the 0.05 and 0.95 quantiles of the sap flow values for each individual tree. Methods used are indicated by different colors in (a) (Constant Heat Dissipation: HD and Trunk Segment Heat Balance: TSHB). A LOESS curve (blue line; grey bands denote the 95% confidence intervals) is used to fit the relationship in (b) to aid visualization. The potential evapotranspiration (PET), which was computed following the Hargreaves-Samani method using the R package "envirem" (Title and Bemmels, 2018), is denoted by the color of the point for each site in (b). Sap flow values of the trees in this study are indicated as triangles (HFD) and squares (LHB). Data from other sites were downloaded from Sapfluxnet (Poyatos et al. 2021). Details of the trees and sites from Sapfluxnet are outlined in the supporting information Table S2.

fraction (e.g., 21, 35 and 48% for the tree #1, #2 and #4) compared to that estimated by HFD.

We observed negative (reversed) flow in all the four study trees, and they were associated with larger discrepancies between estimates from HFD and LHB than the positive flow (Table 1, Fig. 1). Among the study trees, substantial reversed flow was found in tree #2 which was even comparable to the positive flow in magnitude (Fig. 2). The reversed flow usually indicates redistributions of water within plants (Nadezhdina et al., 2010). Our measurement on tree #2 was carefully inspected and the same SFD diurnal pattern was confirmed by another instrument unit (data not shown). Therefore, the possibility of instrumentation issues was excluded. In addition, we also observed significant nocturnal sap flow in tree #3 (Fig. 2), which is a well-documented process that is related to either storage recharge or transpiration at night (e.g., Phillips et al., 2010; Zeppel et al., 2014). Given that the sapwood area (possibly sapwood functionality) does not distribute evenly across different directions of the stem (Børja et al., 2013), we suspect that the reversed and nocturnal flow may vary across directions, which will need to be further studied.

By comparing to sap flow of Norway spruce trees from Sapfluxnet (Poyatos et al., 2021), we found that the four trees in this study represent sap flow magnitude from low to medium (Fig. 6a). The relatively low sap flow is likely associated with the low potential evapotranspiration at the site (512 mm) (Fig. 6b). We also noticed that the magnitude of sap flow estimated by LHB are mostly much lower than the average level from trees of the similar DBH class (Fig. 6b), possibly suggesting an under-estimation of the sap flow.

As a known issue, both methods could introduce large uncertainties when they are used to calculate extremely high sap flow. Nadezhdina (2018) suggested that SFD estimates become unreliable when HFD ratios (R, see Eq. 1) are >13. Trcala and Cermak (2016) claimed that SFD that is >18 $cm^3\ cm^{-2}\ h^{-1}$ tends to be partially underestimated by LHB. However, our data had almost no cases that exceeded these thresholds both in R and SFD. Therefore, we exclude the possibility of high flows

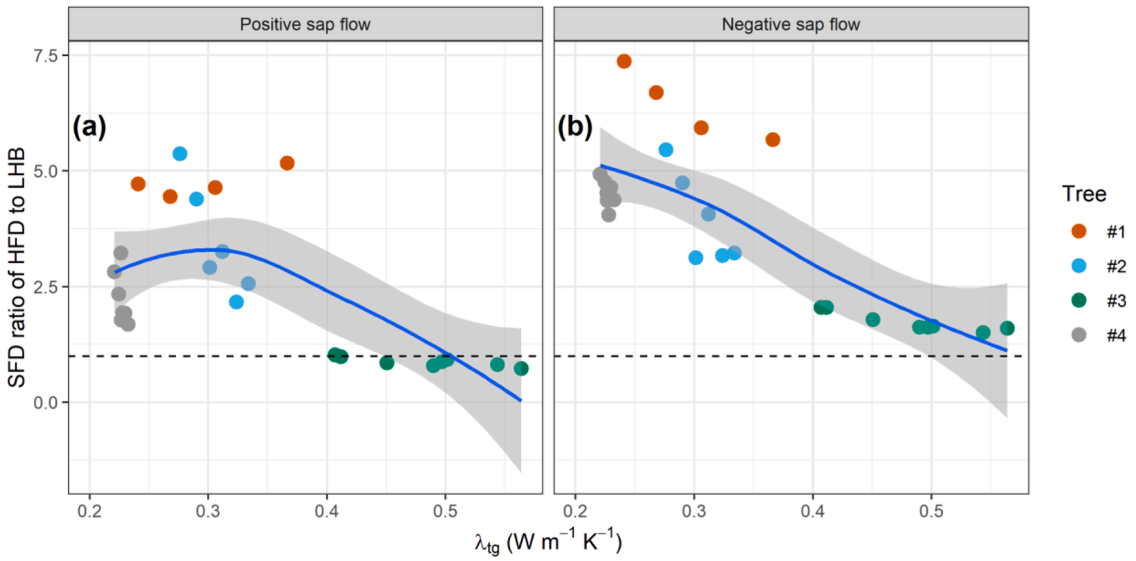

Fig. 7. Slopes of the linear regressions between SFD (positive (a) and negative (b)) estimated by HFD and LHB methods as a function of the wood thermal conductivity along the tangential direction (λ_{tg}, Eq. 4) of the four trees at different depths. The unity ratio is indicated by the dashed line. The LOESS function is used to visualize the relationships as shown by solid blue lines with grey bands (95% confidence intervals).

that caused the discrepancies between the estimates by the two methods.

In addition, Trcala and Cermak (2016) detected significant SFD underestimations in cases where low wood thermal conductivities (i.e., $\lambda_{tg} \leq 0.358$ W m^{-1} K^{-1}) are present. In our case, the calculated mean values of λ_{tg} were 0.24-0.36, 0.28-0.33, 0.39-0.54 and 0.22-0.23 W m^{-1} K^{-1}, respectively, for tree #1, #2, #3 and #4 following Trcala and Cermak (2016). Sonderegger et al. (2011) measured even smaller λ_{tg} in Norway spruce trees that was as low as 0.08 W m^{-1} K^{-1}. We found that smaller λ_{tg} values were indeed associated with lower calculated SFD_{LHB} and larger estimation discrepancies between the two methods (Fig. 7). Wood thermal conductivity is determined by wood properties (e.g., density, porosity), temperature and moisture (MacLean, 1941; Suleiman et al., 1999) and thus can vary across the individual trees. Given that the SFD estimates by LHB are highly sensitive to wood thermal conductivity, we suggest that LHB should not be used for calculations associated with low λ_{tg} values. Applicable corrections for these cases will need to be further investigated. At the same time, given substantial uncertainties (i.e., confidence interval bands in Fig. 7) associated with the relationship between λ_{tg} and the ratio of SFD_{HFD}: SFD_{LHB}, there might be other factors that caused the discrepancies between outputs of the two methods.

The two methods both include empirical parameters in their equations (i.e., k in LHB and D in HFD) where nominal values are recommended. However, we found that the estimated SFD varied strongly with changes in each of the parameters, implying that using a correct parameter value can be crucial for accurate SFD estimates. For the k-value used in LHB, it represents the ratio between the axial and tangential thermal conductivities of the wood. Trcala and Cermak (2016) suggested this value to be 2 following MacLean (1941), who, in fact, reported k-values ranging from 2.25 to 2.75 based on measurements on Douglas-fir and red oak. For Norway spruce, Sonderegger et al. (2011) observed λ_{ax} and λ_{tg} to be 0.25 and 0.08 W m^{-1} K^{-1}, respectively, resulting in a k-value of 3.1. By using this k-value, the SFD_{LHB} would be even smaller which enlarges the discrepancies with SFD_{HFD} for all the study trees, suggesting that the k-value may not be the main reason that led to the discrepancies in our case. Nevertheless, given that the calculated SFD values were highly sensitive to the change of k-value, we suggest that, rather than the nominal value, a case-specific k-value may improve the reliability of SFD estimates from LHB; however, destructive sampling will be required (Sonderegger et al., 2011), which may not be practical in most cases.

The parameter D in the HFD equation Eq. 1 and (2) indicates thermal diffusivity of wood. As suggested by Nadezhdina et al. (2012), a nominal value of 0.0025 cm^2 s^{-1}, which was measured from several conifer trees by Marshall (1958), was taken as default for the calculation. By using this nominal value of D, Steppe et al. (2010) found that HFD estimates underestimated the SFD by an average of 46% (ranging from ~ 2% to 70%) for 9 stem segments of *Fagus Grandifolia* when comparing to gravimetrically measured values. Another study used a higher D value of 0.00299 cm^2 s^{-1} for *F. sylvatica* but resulted in an overestimation of ~11% (Fuchs et al., 2017). For Norway spruce, Sonderegger et al. (2011) reported thermal diffusivity values of 0.0043 and 0.0015 cm^2 s^{-1} along the axial and tangential directions, respectively. Accordingly, a D-value of 0.0036 cm^2 s^{-1} can be derived from the average weighted by the actual axial (1.5 cm) and tangential (0.5 cm) distances of the temperature probs from the heater. This D-value leads to SFD estimates that are 44% greater than the ones calculated with the default D value. As a result, SFD_{HFD} becomes closer to SFD_{LHB} for positive sap flow of the tree #3 but deviates more from SFD_{LHB} for other trees (Fig. 5). Although actual D value may be different from the default nominal value, it is important to note that the HFD is a purely empirical method and thus a more accurate D value does not necessarily lead to a more accurate sap flow estimate. Instead, as claimed by Nadezhdina (2018), the dT_0 (i.e., K-value in Nadezhdina (2018)), which provides the background value of the difference between dT_s and dT_a under the condition of zero sap flow, serves as a correction of the nominal D value. Therefore, rather than to determine the case-specific value for D, the HFD equation should be investigated as a whole for any possible correction (e.g., Vandegehuchte and Steppe, 2012).

In our data, 17% of the measurements had negative HFD ratios (R) (Table S1), which has never been reported in other studies. The negative R was caused by a measured -$dT_{s\text{-}a}$ (for positive SFD) or dT_a (for negative SFD) value that was even greater than the estimated dT_0. In these negative R cases, HFD results in SFD of the opposite sign (e.g., using Eq. (1) for cases with dT_s>0 yields negative SFD) while the LHB equations were not solvable. The outputs from both the methods are problematic in these cases. However, since these negative R values were only found when sap flow was close to zero and mostly during the nighttime (see Fig. S1 for an example of the tree #4), assuming zero sap flow in these occasions would not introduce significant errors to the sap flow budget estimations. According to Nadezhdina (2018), the heat field can be unstable during transitional period when the flow of opposite direction starts to develop but is not fully established. These measurement uncertainties associated with low sap flow may be partly responsible for the negative R values. In addition, in this study, pulse heating, rather than the typical constant heating, was used due to limited power from solar panels and whether the negative R values are the effect of noise introduced by our heating scheme will need to be investigated in the future.

Even though LHB is developed based on mechanistic (physical) theories, it has been seldom applied in sap flow calculations so far. Our study highlights the high sensitivity of the sap flow output in the LHB calculation to wood thermal conductivity and the associated empirical parameter k. Since it significantly underestimates sap flow in trees with low thermal conductivity, application of the method should be carefully evaluated. By contrast, HFD approach generated more reasonable sap flow values for trees with low thermal conductivities. However, without referencing to the corresponding "true" sap flow rates, we are not able to evaluate the accuracy of the HFD approach. Future studies that compare the outputs from these two methods with results from a more direct measuring approach, such as the gravimetrical method (Fuchs et al., 2017; Steppe et al., 2010), are encouraged to further improve the parameterization of the two methods for different trees under various environmental conditions.

Declaration of Competing Interest

The authors declare that they have no known competing financial interests or personal relationships that could have appeared to influence the work reported in this paper.

Acknowledgments

The study is supported by the Research Council of Norway grant 294948 and by the Framsenter grant A-340216. We would like to thank Dr. Nadezhda Nadezhdina for her great suggestions in data processing, interpretation, trouble shooting and manuscript revision.

Supplementary materials

Supplementary material associated with this article can be found, in the online version, at doi:10.1016/j.agrformet.2022.108974.

References

Becker, P., 1996. Sap flow in Bornean heath and dipterocarp forest trees during wet and dry periods. Tree Physiol. 16 (1-2), 295–299.
Børja, I., et al., 2013. Sap flow dynamics as a diagnostic tool in Norway spruce. Acta Hortic. 991, 31–36.
Cermak, J., Kucera, J., Nadezhdina, N., 2004. Sap flow measurements with some thermodynamic methods, flow integration within trees and scaling up from sample trees to entire forest stands. Trees-Struct Funct 18 (5), 529–546.
David, T.S., et al., 2012. Hydraulic connectivity from roots to branches depicted through sap flow: analysis on a Quercus suber tree. Funct. Plant Biol. 39 (2), 103–115.
Fuchs, S., Leuschner, C., Link, R., Coners, H., Schuldt, B., 2017. Calibration and comparison of thermal dissipation, heat ratio and heat field deformation sap flow probes for diffuse-porous trees. Agric. For. Meteorol. 244, 151–161.
Kume, T., et al., 2007. Impact of soil drought on sap flow and water status of evergreen trees in a tropical monsoon forest in northern Thailand. Forest Ecol. Manag. 238 (1-3), 220–230.
MacLean, J.D., 1941. Thermal conductivity of wood. Heat Pipe Air Condit. 13, 380–391.
Marshall, D.C., 1958. Measurement of Sap Flow in Conifers by Heat Transport. Plant Physiol. 33 (6), 385–396.
Nadezhdina, N., 2018. Revisiting the Heat Field Deformation (HFD) method for measuring sap flow. Iforest 11, 118–130.
Nadezhdina, N., Al-Okaishi, A., Madera, P., 2018. Sap flow measurements in a socotra dragon's blood tree (Dracaena cinnabari) in its area of origin. Trop Plant Biol 11 (3-4), 107–118.
Nadezhdina, N., Cermak, J., Gasparek, J., Nadezhdin, V., Prax, A., 2006. Vertical and horizontal water redistribution in Norway spruce (Picea abies) roots in the Moravian Upland. Tree Physiol. 26 (10), 1277–1288.
Nadezhdina, N., et al., 2010. Trees never rest: the multiple facets of hydraulic redistribution. Ecohydrology 3 (4), 431–444.
Nadezhdina, N., Vandegehuchte, M.W., Steppe, K., 2012. Sap flux density measurements based on the heat field deformation method. Trees-Struct. Funct. 26 (5), 1439–1448.
O'Brien, J.J., Oberbauer, S.F., Clark, D.B., 2004. Whole tree xylem sap flow responses to multiple environmental variables in a wet tropical forest. Plant Cell Environ. 27 (5), 551–567.
Phillips, N.G., Lewis, J.D., Logan, B.A., Tissue, D.T., 2010. Inter- and intra-specific variation in nocturnal water transport in Eucalyptus. Tree Physiol. 30 (5), 586–596.
Poyatos, R., et al., 2021. Global transpiration data from sap flow measurements: the SAPFLUXNET database. Earth Syst. Sci. Data 13 (6), 2607–2649.
R Development Core Team, 2021. R: A Language and Environment for Statistical Computing. R Foundation for Statistical Computing, Vienna, Austria. URL. http://www.R-project.org/.
Smith, D.M., Allen, S.J., 1996. Measurement of sap flow in plant stems. J. Exp. Bot. 47 (305), 1833–1844.
Sonderegger, W., Hering, S., Niemz, P., 2011. Thermal behaviour of Norway spruce and European beech in and between the principal anatomical directions. Holzforschung 65 (3), 369–375.
Steppe, K., De Pauw, D.J.W., Doody, T.M., Teskey, R.O., 2010. A comparison of sap flux density using thermal dissipation, heat pulse velocity and heat field deformation methods. Agric. For. Meteorol. 150 (7-8), 1046–1056.
Suleiman, B.M., Larfeldt, J., Leckner, B., Gustavsson, M., 1999. Thermal conductivity and diffusivity of wood. Wood Sci. Technol. 33 (6), 465–473.
Title, P.O., Bemmels, J.B., 2018. ENVIREM: an expanded set of bioclimatic and topographic variables increases flexibility and improves performance of ecological niche modeling. Ecography 41 (2), 291–307.
Trcala, M., Cermak, J., 2016. A new heat balance equation for sap flow calculation during continuous linear heating in tree sapwood. Appl. Therm. Eng. 102, 532–538.
Vandegehuchte, M.W., Steppe, K., 2012. Interpreting the Heat Field Deformation method: erroneous use of thermal diffusivity and improved correlation between temperature ratio and sap flux density. Agric. For. Meteorol. 162, 91–97.
Wickham, H., 2016. ggplot2: Elegant Graphics for Data Analysis. Springer-Verlag, New York.
Zeppel, M.J.B., Lewis, J.D., Phillips, N.G., Tissue, D.T., 2014. Consequences of nocturnal water loss: a synthesis of regulating factors and implications for capacitance, embolism and use in models. Tree Physiol. 34 (10), 1047–1055.